

SANDIA REPORT

SAND2014-20011

Unlimited Release

Printed September 2014

Injection of a Phase Modulated Source into the Z-Beamlet Laser for Increased Energy Extraction

Patrick K. Rambo, Darrell J. Armstrong, Jens Schwarz, Ian C. Smith, Jonathan Shores, C. Shane Speas, and John L. Porter

Prepared by
Sandia National Laboratories
Albuquerque, New Mexico 87185 and Livermore, California 94550

Sandia National Laboratories is a multi-program laboratory managed and operated by Sandia Corporation, a wholly owned subsidiary of Lockheed Martin Corporation, for the U.S. Department of Energy's National Nuclear Security Administration under contract DE-AC04-94AL85000.

Approved for public release; further dissemination unlimited.



Sandia National Laboratories

Issued by Sandia National Laboratories, operated for the United States Department of Energy by Sandia Corporation.

NOTICE: This report was prepared as an account of work sponsored by an agency of the United States Government. Neither the United States Government, nor any agency thereof, nor any of their employees, nor any of their contractors, subcontractors, or their employees, make any warranty, express or implied, or assume any legal liability or responsibility for the accuracy, completeness, or usefulness of any information, apparatus, product, or process disclosed, or represent that its use would not infringe privately owned rights. Reference herein to any specific commercial product, process, or service by trade name, trademark, manufacturer, or otherwise, does not necessarily constitute or imply its endorsement, recommendation, or favoring by the United States Government, any agency thereof, or any of their contractors or subcontractors. The views and opinions expressed herein do not necessarily state or reflect those of the United States Government, any agency thereof, or any of their contractors.

Printed in the United States of America. This report has been reproduced directly from the best available copy.

Available to DOE and DOE contractors from
U.S. Department of Energy
Office of Scientific and Technical Information
P.O. Box 62
Oak Ridge, TN 37831

Telephone: (865) 576-8401
Facsimile: (865) 576-5728
E-Mail: reports@adonis.osti.gov
Online ordering: <http://www.osti.gov/bridge>

Available to the public from
U.S. Department of Commerce
National Technical Information Service
5285 Port Royal Rd
Springfield, VA 22161

Telephone: (800) 553-6847
Facsimile: (703) 605-6900
E-Mail: orders@ntis.fedworld.gov
Online ordering: <http://www.ntis.gov/help/ordermethods.asp?loc=7-4-0#online>



Injection of a Phase Modulated Source into the Z-Beamlet Laser for Increased Energy Extraction

Patrick K. Rambo, Darrell J. Armstrong, Jens Schwarz, Ian C. Smith,
Jonathan Shores, C. Shane Speas, and John L. Porter

Laser Operations and Engineering (Org. 1682)
Sandia National Laboratories
P.O. Box 5800
Albuquerque, New Mexico 87185-MS1197

Abstract

The Z-Beamlet laser has been operating at Sandia National Laboratories since 2001 to provide a source of laser-generated x-rays for radiography of events on the Z-Accelerator. Changes in desired operational scope have necessitated the increase in pulse duration and energy available from the laser system. This is enabled via the addition of a phase modulated seed laser as an alternative front-end. The practical aspects of deployment are discussed here.

Acknowledgment

We would like to acknowledge Briggs Atherton for his guidance during the very early stages of this work.

Contents

Introduction 9

Transverse SBS and Associated Operational Risks 11

The PM Seed Source and Failsafe 14

The AM Control 17

High Energy Data 23

Conclusions 27

References 28

List of Figures

1	Explanation of PM impact upon transverse SBS. For a single frequency (0 order) sideband (i.e. no PM), the spectral power remains concentrated, with the power exceeding a threshold level that places the system at risk for a transverse SBS event (as seen on the left side). As PM is added, the distribution of the spectral power into a sufficient number of spectral sidelobes reduces the power of any individual lobe below the threshold level, thus keeping the system safe from transverse SBS (as seen on the right side). β is a representative modulation index for the phase modulator used in this example.	12
2	Schematic of the PM system.	15
3	Schematic of the PM failsafe.	16
4	Impact of PZ fiber dispersion on AM. (a) Measurement of a 1 ns pulse coming out of a 30 m PZ fiber without any PM on the pulse. (b) Corresponding measurement with the PM system enabled.	18
5	Impact of amplifiers on AM. (a) Measurement of a 1 ns pulse after a 30 m PZ fiber and the regenerative amplifier with PM on the pulse. (b) Comparison of the amplitudes of the Fast Fourier Transform of the regenerative amplifier input and output. (c) Measurement of a 1 ns pulse after a 30 m PZ fiber, the regenerative amplifier, and the 4-pass rod amplifier with PM on the pulse. (d) Comparison of the amplitudes of the Fast Fourier Transform of the 4-pass rod amplifier input and output.	19
6	Grating compressor for pre-compensation of dispersion for PM system. G1 and G2 are the gratings, HRM is the hollow roof mirror which shifts the beam vertically down to facilitate beam pickoff, HWP is a half wave plate to set the polarization to match the transmission axis for the subsequent PZ fiber, and FOC is the fiber-optic coupler into the PZ fiber.	20
7	Pre-compensation of dispersion of PZ fiber for PM system. (a) Resulting 30 m PZ fiber output for no PM (and therefore no possible AM) on an 8 ns pulse. (b) Corresponding 30 m PZ fiber output with pre-compensated PM.	21
8	Compensation of spectral amplitude changes in the regenerative amplifier using a BRF.	21
9	Full compensation of spectral amplitude and phase changes in the 4-pass rod amplifier.	22

10	Fast photodiode output at 2ω for a low energy full system shot (below SBS threshold). The left trace (a) is the normalized fast photodiode data while the right traces (b) is the corresponding Fourier transform.	23
11	Fast photodiode output at 1ω for three sequential ZBL shots. The left traces (a,c,e) are the normalized fast photodiode data while the right traces (b,d,f) are the corresponding Fourier transforms. The 1ω energies were: 5923 J for B14052801, 5784 J for B14052803, and 5891 J for B14060301.	25
12	L3 scatter photodiode measurement at 1ω . (a) Representative photodiode trace. (b) Plot of normalized photodiode integral versus energy.	26

Introduction

The Z-Beamlet Laser (ZBL) began operations at Sandia National Laboratories (SNL) in 2001 with the primary mission of x-ray radiography [1]. In this effort, the laser is focused onto a metallic foil to generate a burst of x-rays for radiography (also referred to as backlighting) of events in Sandia's Z-Accelerator. This mission requires balancing high laser energy needs (for high x-ray conversion) with appropriately short pulse duration requirements so as to minimize motional blurring in fast hydrodynamic events. Initial ZBL operation employed 300 ps pulses but the energy had to be restricted to less than 1 kJ at 1054 nm to avoid intensity-dependent damage effects in the laser system. Increased laser energy would necessitate increased laser pulsewidth. As the system evolved, an operational point of around 3.5 kJ at 1054 nm in 2 ns (with subsequent second harmonic conversion to around 2.5 kJ at 527 nm) was determined to provide acceptable quality radiographs. However, new initiatives such as MagLIF [2] require more energy without the same temporal constraints. In these new scenarios beyond the backlighting mission, the goal is simply to deliver as much energy as possible to a target. To consider this effort, there are a variety of limiting factors which prevent arbitrarily increasing the pulsewidth. These include:

- *Arbitrary Waveform Generator (AWG) Record Length:* The current device, used in setting the front-end seed waveform for the regenerative amplifier and subsequent amplifiers, is limited to 11 ns of record length. Other models could be procured given time and budget but the increase in record length might come at the expense of the high temporal resolution that our current unit provides.
- *Regenerative Amplifier Round Trip Time:* The first amplifier in the chain, the regenerative amplifier restricts injected pulsed waveform length to 9 ns, based upon the round-trip time of the cavity (14 ns) less the on-off time of the switching cavity Pockels cells (5 ns). The cavity length and associated lifetime can be increased with modest design changes but a longer cavity would most likely be less stable and thus less desirable operationally.
- *Pinhole Closure Associated with Existing ZBL Cavity and Transport Spatial Filter Pinholes:* When hit by the spatial wings of the laser pulse, a metallic pinhole in one of the spatial filter focal planes can create a plasma blow-off that jets inward toward the pinhole center, obscuring the latter part of the pulse temporally (within 5 to 6 ns) [3,4]. Elaborate conical pinholes can mitigate the effect but require budget and time to implement.
- *Transverse Stimulated Brillouin Scatter (SBS):* Transverse SBS is a nonlinear optical effect associated with large aperture high intensity lasers which can reduce laser transmission and cause damage to the system optics for timescales beyond 2 to 3 ns [5,6].

There are additional energy limiting constraints, some of which are temporally coupled:

- *Laser-Induced Damage Thresholds*: Material damage can occur with high intensity lasers but typically the damage fluence level increases with pulsewidth τ [7]. Since the damage fluence often scales as $\sqrt{\tau}$ and saturation effects keep the increases in laser fluence from scaling linearly with τ , the likelihood of damage as we increase the energy and duration is likely similar to the situation in traditional laser operations.
- *B-Integral (Non-linear phase accumulation)*: Nonlinear phase accumulation can lead to local focusing which increases the present intensity above laser-induced damage thresholds. Calculations [8] estimate maximum allowable intensities in the 1 to 3 GW/cm² region, depending on pulsewidth. These calculations indicate how long the pulse must be made.
- *Energy Storage in the Main Amplifiers*: The optical pumping of the main amplifier units deposits a limited amount of energy which can be extracted. This is typically of order 550-600 J per amplifier unit (which is a single slab).

With all of these considerations in mind, transverse SBS is the limiting factor which starts at the shortest pulse durations. As such, transverse SBS must be addressed first in order to expand the pulsewidth and thus increase the energy. To appropriately tackle this problem, we must understand the phenomenon and determine when the effect is a problem. Subsequently, we develop a mitigation technology based on those used in other high energy lasers within the inertial confinement fusion (ICF) community.

Transverse SBS and Associated Operational Risks

Transverse SBS is a detrimental nonlinear effect in high energy, large aperture laser systems [5, 6]. In transverse SBS, a high intensity laser beam generates acoustic waves within a medium (such as glass) of sufficiently large aperture that the acoustic waves can amplify, leading to optical scattering. Such scatter in turn creates losses along with instability and damage, although there is also indication that the acoustic wave itself can cause damage. Even without damage, SBS energy losses will prevent delivery of the full energy to target, rendering a given laser system less effective. The measured 3ω (or third harmonic of the Nd:Glass laser system at 351 nm) SBS threshold is $2.3 \text{ J}\cdot\text{ns}/\text{cm}^2$ [6]. Unmeasured λ^2 scaling implies [6] the 1ω (or fundamental wavelength of the laser at 1054 nm) threshold is $20.7 \text{ J}\cdot\text{ns}/\text{cm}^2$. Using this value and current nominal ZBL values for a pulsewidth of 2.5 ns and an area of 1000 cm^2 , a threshold transverse SBS energy value at 1ω is determined to be 8.3 kJ. This not a problem as the energy far exceeds the stored energy and B-integral limitations. However, at 4.0 ns, the same energy threshold shifts to 5.2 kJ, which could pose a problem since other factors do not limit the system from reaching this energy. Note that, in conjunction with a sufficiently large beamsizes, the longer laser pulse duration allows more time for the transverse nonlinear effect to develop and propagate. Essentially, current operational modes at less than 2.5 ns are fine but going beyond this pulsewidth will require new machine safety technologies.

The transverse SBS can be suppressed by the addition of multiple frequency sidebands (via an electro-optic phase modulator) on the laser pulse. The basic concept of using phase modulation (PM) is to distribute the energy from a single laser frequency which could be above the transverse SBS threshold to many nearby frequency lobes that have individual amplitudes below the SBS power threshold, as shown in Fig. 1. Based upon the nature of the transverse SBS process, these lobes do not interact constructively with each other (as long as the frequency spacing exceeds the reciprocal of the SBS decay time). This approach (known as SBS suppression or SBSS) has been used at a variety of large ICF lasers successfully [9–19]. These sidebands are easily within 1 nm bandwidth, lying within both the gain bandwidth of the Nd:Phosphate glass amplifying medium and the acceptance bandwidth of the frequency doubling and tripling crystals used for the target interactions in ICF systems.

The introduction of a PM laser pulse to increase the laser pulsewidth and energy, while mitigating the transverse SBS hazard, introduces three other key risks. The first risk is simply that, by getting the extra energy that we want, more laser damage will occur in the amplifier chain, leading to increased optics consumption. Local spatio-temporal intensity spikes already can create damage on ZBL optics based upon bulk or surface damage thresholds (which can be reduced even further if local contaminants are present). Increased laser energy will only increase the likelihood of such operational damage. At higher energies, a better supply chain for spare optics is needed in addition to better cleanroom conditions and protocols. The second risk is induced amplitude modulation (AM). Subtle dispersion and/or spectral modifications with a PM pulse can lead to amplitude modulation imprinted on the pulse [10, 11, 13–19]. The resulting temporal spikes imprinted upon the pulse can

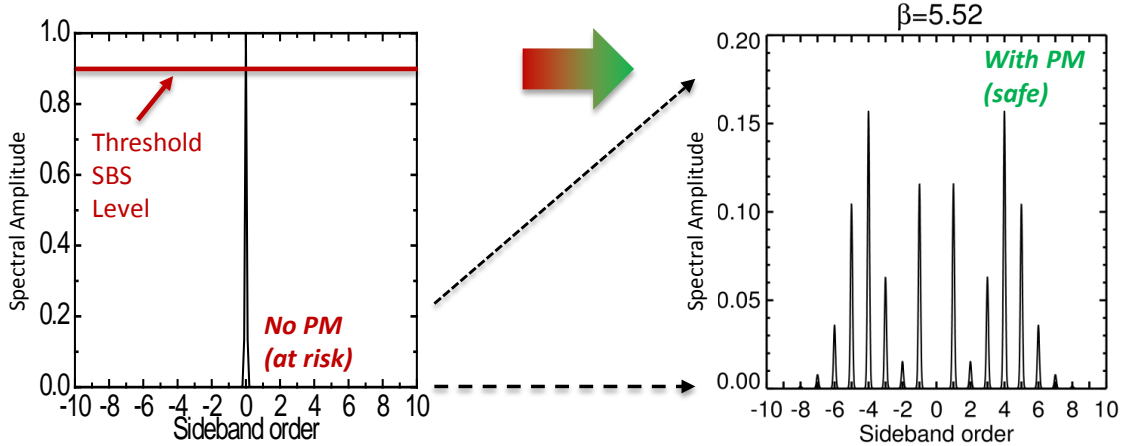


Figure 1. Explanation of PM impact upon transverse SBS. For a single frequency (0 order) sideband (i.e. no PM), the spectral power remains concentrated, with the power exceeding a threshold level that places the system at risk for a transverse SBS event (as seen on the left side). As PM is added, the distribution of the spectral power into a sufficient number of spectral sidelobes reduces the power of any individual lobe below the threshold level, thus keeping the system safe from transverse SBS (as seen on the right side). β is a representative modulation index for the phase modulator used in this example.

result in optical damage or can cause transverse SBS. At the Omega-EP facility [19], the AM budget is 20% peak-to-valley noise, as measured at the regenerative amplifier output. Such AM risk can be mitigated via AM compensation techniques for spectral amplitude and phase (i.e. dispersion) control. Finally, there is the risk of accidentally seeding of the main amplifiers with a non-PM pulse. If the seed pulse providing PM light should fail in its phase modulation and instead provide single frequency light, all of the transverse SBS risks are present. A system failsafe is required to prevent this.

To underscore the impact of the PM seed source and the importance of the failsafe, consider an incident that occurred with ZBL in its prior incarnation as Beamlet, the National Ignition Facility prototype operated at Lawrence Livermore National Laboratories (LLNL) in the mid-1990's. Prior to transfer from LLNL to SNL, the Beamlet laser suffered significant damage on September 17, 1996 during an attempted laser shot [20]. The shot B6091723 was 15.3 kJ of 1ω energy with a 20 ns shaped pulse (in a larger area beam than used by ZBL at SNL). Note that the larger beam size, significantly longer pulse, and the presence of booster amplifiers (not currently at ZBL) allowed a much higher energy. A pulsed PM system had been implemented to impart modulation upon a pulsed laser seed. However, transverse SBS occurred on shot in the round L3 lens which served as a vacuum barrier in the transport spatial filter (TSF). The transverse SBS light created in L3 was absorbed by the o-ring seal at the lens edge and a subsequent acoustic wave was generated. This wave converged at the lens center due to its circular geometry, causing L3 to crack into multiple pieces and implode. The L3 lens and adjacent booster amplifier were critically damaged. The root

cause was insufficient phase modulation due to inappropriate synchronization between the pulsed PM hardware and the pulsed laser seed. LLNL corrective actions included:

- *The implementation of square lenses for vacuum barriers:* This prevents the focusing of any acoustic waves.
- *The use of lower tensile stresses at relevant lenses:* By increasing the thickness of lenses and vacuum barriers slightly, the optic can stay within a two-piece fracture limit such that implosions (which are caused by fragmentation into 3 or more pieces) cannot occur [21].
- *The use of improved diagnostics, checklists, and failsafes for the PM aspect of operations:* While the previous corrective actions prevent vacuum barrier implosions, the implementation of operational elements was intended to prevent transverse SBS at all [9], which can cause significant energy losses in the tail of the pulse.

Based upon these considerations, an implementation plan (including risk mitigations) for the new transverse SBS suppression system implemented at SNL requires the following changes to occur:

- *Add a phase modulated (PM) laser seed source:* This employs constant PM on the continuous wave laser source prior to pulse generation, which in turn avoids any possible synchronization issue as at LLNL.
- *Add a fast failsafe:* A failsafe eliminates the possibility of seeding of the main amplifiers with unmodulated light if the PM should fault. A latch-and-hold circuit on the failsafe system avoids spurious reset. This latched failsafe can provide a “hold” command to ZBL’s control system.
- *Apply amplitude modulation (AM) Compensation:* A dispersion compensator unit (grating compressor) and spectral filter unit (birefringent filter) are inserted at the relevant positions to minimize the damage risk from AM.
- *Exchange Current Damaged ZBL Optics:* Normal accumulated local damage to the M4, M5, and L3 optics within the ZBL beam train has existed and has allowed operating within the normal operational parameter space. However, under even higher laser fluences, such local sites could pose catastrophic damage initiation (especially for L3) if not replaced. This effort was performed under normal maintenance.

Per “safety in depth”, ZBL maintained existing engineered safety developed previously for mitigating the transverse SBS hazard, namely the use of all square lenses in the high energy part of the beam train and the use of thick lenses designed to operate within a two-piece fracture limit.

The PM Seed Source and Failsafe

Phase modulation of a laser by itself is almost trivial. High-bandwidth fiber-coupled low-power LiNbO_3 waveguide modulators work well and are easy to use. To get PM seed laser light for an amplifier chain, one simply adds one to the seed laser system where average optical power is below 25 mW at 1054 nm. Although other facilities have shown that one can use lower frequency modulations of around 3 GHz for SBSS, the ZBL facility has chosen to use a higher frequency of around 15 GHz in consideration of possible smoothing by spectral dispersion (SSD) applications. While the modulation process is somewhat straightforward, the system gets significantly complicated when considering the PM failsafe. The details of the PM system and failsafe are found in [22].

The PM failsafe needs to have a high speed response to prevent a failure from seeding the chain with unmodulated laser light. Ideally, the failsafe also has continuous monitoring without reference to any clock. As such, optical heterodyne detection is a good choice to achieve high-bandwidth continuous monitoring. The PM optical system (see Fig. 2) starts with a low power (80 mW) single-longitudinal mode continuous wave fiber laser operating at 1054 nm. A 50-50 fiber splitter divides the beam, routing half to a 14.8 GHz phase modulator and half to a 12.8 GHz modulator. The output of the 12.8 GHz modulator is outcoupled, collimated, and goes through a confocal etalon locked to the first order sideband. This first order sideband is re-coupled into a fiber and is then combined with 10% of the 14.8 GHz modulated light to establish a heterodyne beat note. The other 90% of the 14.8 GHz modulated light goes through a fiber amplifier to reach the 1 W level before temporal chopping, dispersion compensation (see below), electro-optic pulseshaping (driven by an AWG), and delivery with a PZ fiber to the regenerative amplifier.

The heterodyne beat note is detected with an 8 GHz bandwidth detector and enters the electrical portion of the failsafe. This electrical section converts the heterodyne signal to TTL failsafe trigger by RF power detection (see Fig. 3). Doing so eliminates the need for phase-sensitive electronic demodulation at the PM frequency of 14.8 GHz, with frequency down-conversion being achieved optically by amplitude splitting and recombination of a stable laser source which has no slow-drift interference from carriers. This absence of slow-drift from carrier interference occurs only by using two modulation indices that have no carriers. The system is designed for speed, with RF components responding to a change in heterodyne signal in about 14 ns and the overall system responding to change in heterodyne signal (from point A to B in Fig. 3) in about 36 ns. Note that, as an additional precaution, the failsafe also incorporates a well behaved high-bandwidth latch-and-hold that kills the system until reset by a human operator. This latched failsafe protects a ZBL shot by interrupting the regenerative amplifier output at the slicer Pockels cell used just after the amplifier. Under a fault condition, the output of a delay generator (Stanford Research Systems DG535) used to trigger this Pockels cell is inhibited, preventing the regeneratively amplified pulse from going through the slicer Pockels cell. In turn, this prevents seeding the rest of the amplifier chain. With a common optical starting point in the PM seed laser, the light which propagates to the regenerative amplifier and then circulates around it has a much longer delay time than light which initiates a fault and is converted to an electrical inhibit signal for the slicer Pockels

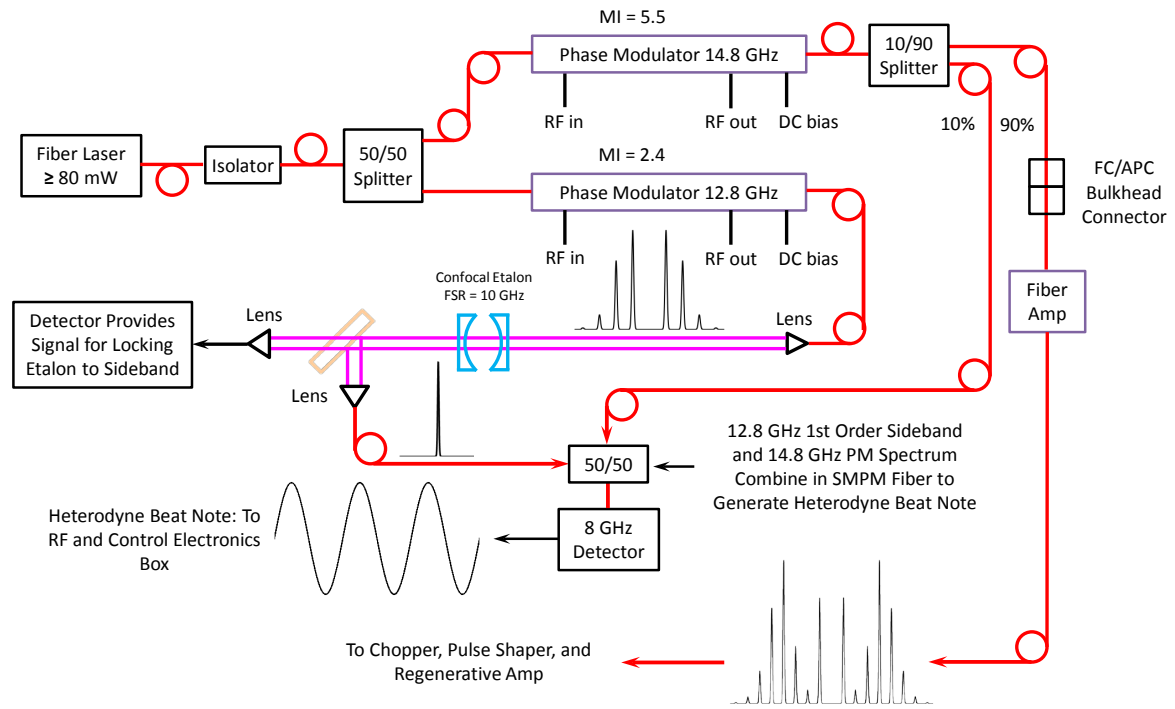


Figure 2. Schematic of the PM system.

cell. As such, the failsafe covers all key failure conditions and maintains machine safety.

Because of the latch-and-hold circuit, the failsafe output can be incorporated at a later date into the LabView-based ZBL control system to inhibit the firing of the main amplifiers if a fault occurs. This will not only prevent the seeding of the laser system with detrimental unmodulated light but can prevent a shot on ZBL (and potentially the Z-Accelerator). While the former issue is driven by machine safety, the latter issue is driven by facility schedule and cost issues.

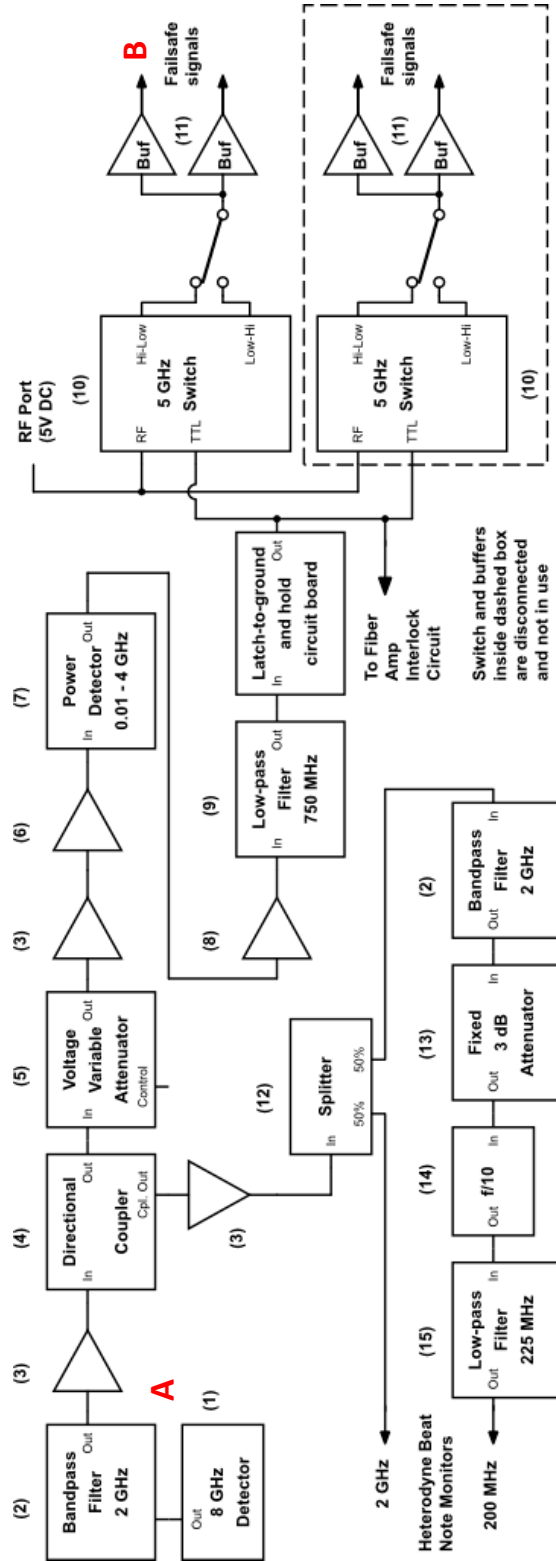


Figure 3. Schematic of the PM failsafe.

The AM Control

As mentioned, the control of AM is accomplished through control of spectral amplitude and spectral phase (i.e. dispersion) in various places. To know what amounts of AM were present, pulses were checked for AM at various locations by fiber coupling the laser light at the area of investigation into a 50 GHz photo diode coupled to a 20 GHz oscilloscope. Note that this detection method was cross-checked with a femtosecond-scale streak camera in order to verify no higher frequency effects existed which the photodiode and oscilloscope could not detect. Figure 4 shows the laser temporal pulse shape of a single 1 ns FWHM square pulse prior to regenerative amplifier injection (but after the 30 m PZ fiber run from the PM seed). The left part of the figure shows the diode trace with the PM system off while the right part of the figure shows the pulse with the PM on. In the case of no PM, there is no bandwidth for dispersion to impact therefore any detected “modulation” is simply random noise. In the case of PM being on, AM is clearly observed from the dispersion of the fiber as no mechanism for shaping the spectral amplitude exists in the fiber.

Subsequent checks were conducted after the regenerative amplifier and after the 4-pass rod amplifier (see Fig. 5), with the AM growing worse after the regenerative amplifier. Note that the Fourier transform of the photodiode data, shown in Fig. 5b and d, has a spike at the modulation frequency when PM is present, with the amplitude of the spike growing with the AM level. In these amplifier cases, the source of AM could be either spectral amplitude manipulation or dispersion. However, as the total amount of glass is less in these sections than in the fiber and the AM contribution is large, one can surmise that this AM is due to a non-uniform gain profile that differentially amplifies the various frequency components of the PM pulse, most likely from gain narrowing and/or slight shifts between the seed wavelengths and the spectral gain envelope. One can see from the Fig. 5c and d that the peak-to-valley modulation at the rod amp exit is similar to the injected pulse from the regenerative amplifier output (or maybe even a little better). This effect is most likely due to lower gain narrowing in the rod amplifier since the gain in the rod amplifier is $\sim 5 \times 10^3$ times as opposed to the $\sim 1 \times 10^6$ times gain in the regenerative amplifier. An alternative explanation would be that the rod amplifier medium is better matched to the seed wavelengths and thus provides more spectrally symmetric gain.

Regarding compensatory measures, we started by considering dispersion. Such compensation can be accomplished via a traditional grating compressor [19]. To design the compressor, we first must estimate the amount of dispersion (specifically the 2nd order dispersion or group velocity dispersion) which must be compensated. To do this, we look at the amount of and types of glass in the system. Based upon the literature, polarizing (PZ) fiber is used to avoid FM-to-AM conversion [10]. In our system, a minimum length of 30 m of PZ fiber is used to transport the seed pulse from the PM source to the amplifiers. In the following amplifier stages, the pulse encounters approximately 2.5 m of glass in the regenerative amplifier, 2.5 m of glass in the 4-pass rod amplifier, and 3.0 m of glass in the 4-pass main slab amplifier (of which all values are predominantly the Nd:Phosphate glass amplifier medium). As such, we begin by trying to compensate the PZ fused silica fiber since it is dominant. We use the Sellemeier equation for fused silica to calculate a group velocity dis-

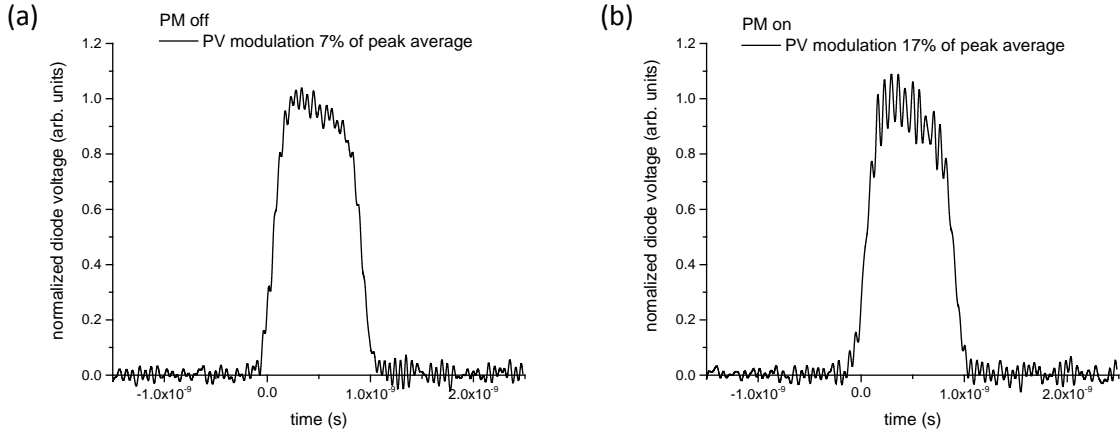


Figure 4. Impact of PZ fiber dispersion on AM. (a) Measurement of a 1 ns pulse coming out of a 30 m PZ fiber without any PM on the pulse. (b) Corresponding measurement with the PM system enabled.

persion of $d^2k/d\omega^2=559 \text{ fs}^2/\text{cm}$ at 1054 nm, leading to a phase term of $d^2\phi/d\omega^2= d^2k/d\omega^2z = 1.68 \times 10^6 \text{ fs}^2$. A double-pass Treacy grating compressor (i.e. 4 grating diffractions) using 14801/mm gold gratings with 56.53° input angle-of-incidence (46.53° diffracted angle) and a grating separation of 8.75 cm is designed to give an oppositely signed $d^2\phi/d\omega^2$ for compensation at 1054 nm. Adjustability from 8 to 11 cm separation will allow the appropriate range to be covered for the overall system. The system is rack mounted with the PM source, providing pre-compensation for dispersion (see Fig. 6), similar to the approach used in employed in the Omega-EP facility [19]. Figure 7 compares the resulting propagation of a non-PM pulse with a dispersion-compensated PM pulse just before the regenerative amplifier and after the 30 m of PZ fiber (as in Fig. 4 but with a longer 8 ns pulsewidth). With pre-compensation and the PM on, instead of a 10% AM increase from the PM off case as in Fig. 4, one only detects a 2.7% AM increase over the PM off case (which is hard to distinguish from the noise level).

Checks of the pulse (using the same methodology) after the regenerative amplifier showed the return of AM at levels similar to those coming out of the uncompensated PZ fiber before the amplifier. Since the amount of glass in the regenerative amplifier is significantly less than the PZ fiber, the source of this amount of AM cannot be dispersion but must be due to spectral amplitude changes (as mentioned above). Adjusting the grating compressor to minimize the AM signal after the regenerative amplifier verified this. Other facilities have used a variety of methods to compensate the AM from spectral amplitude changes but the easiest to implement appears to be the birefringent filter (BRF) employed at the Omega-EP facility [19]. Unless specially designed, BRF's in conjunction with a polarizer can be used to create modulations in spectral transmission which usually have modest depth and are sinusoidal as a function of wavelength. This modest compensation has lead us to using an anti-reflection coated BRF intracavity in the regenerative amplifier, as is common in the

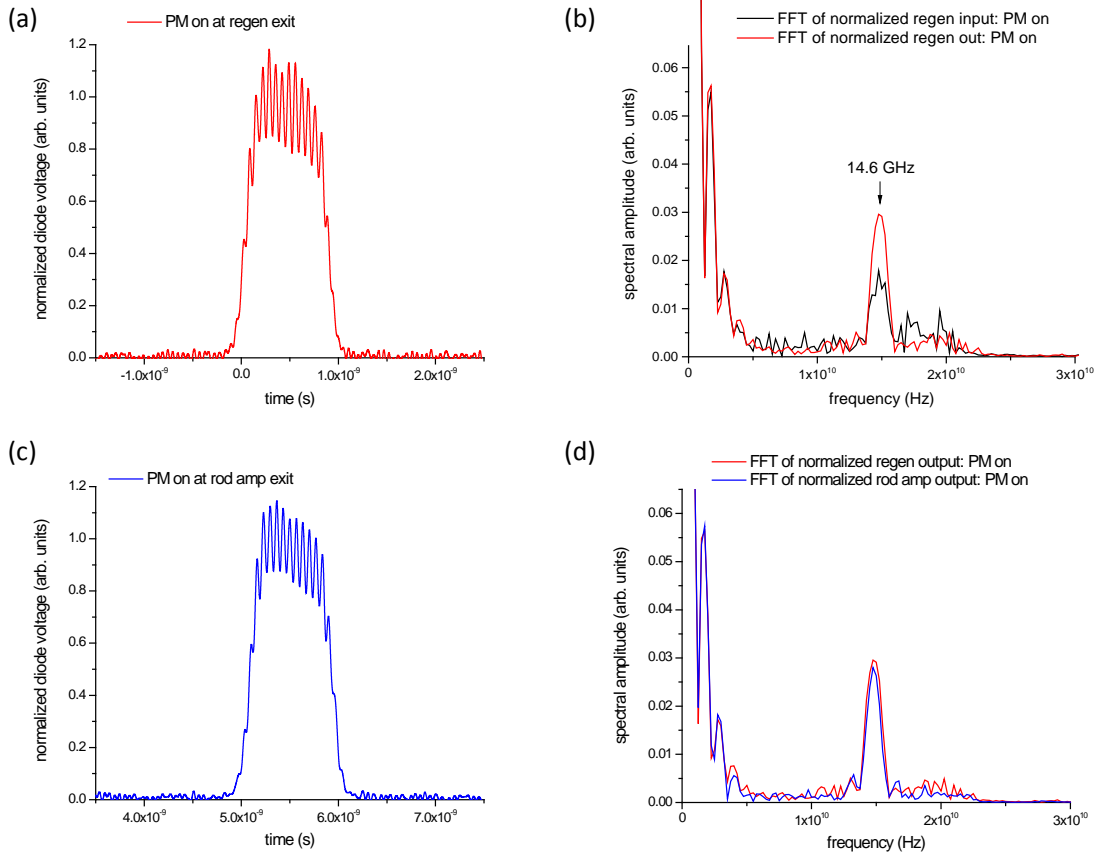


Figure 5. Impact of amplifiers on AM. (a) Measurement of a 1 ns pulse after a 30 m PZ fiber and the regenerative amplifier with PM on the pulse. (b) Comparison of the amplitudes of the Fast Fourier Transform of the regenerative amplifier input and output. (c) Measurement of a 1 ns pulse after a 30 m PZ fiber, the regenerative amplifier, and the 4-pass rod amplifier with PM on the pulse. (d) Comparison of the amplitudes of the Fast Fourier Transform of the 4-pass rod amplifier input and output.

ultrashort pulse laser community [23] rather than as a pre-compensator (as in [19]). The resulting AM compensation from both the BRF and grating compressor (as seen after the regenerative amplifier) is quite good (see Fig. 8).

As mentioned, the rod amplifier has lower gain and dispersion than earlier elements, which leads to nice compensation of AM after the 4-pass rod amplifier without any changes from the settings from the regenerative amplifier (see Fig. 9). Based upon this operational environment, the presence of AM in the front-end of the amplifier chain can be appropriately dealt with.

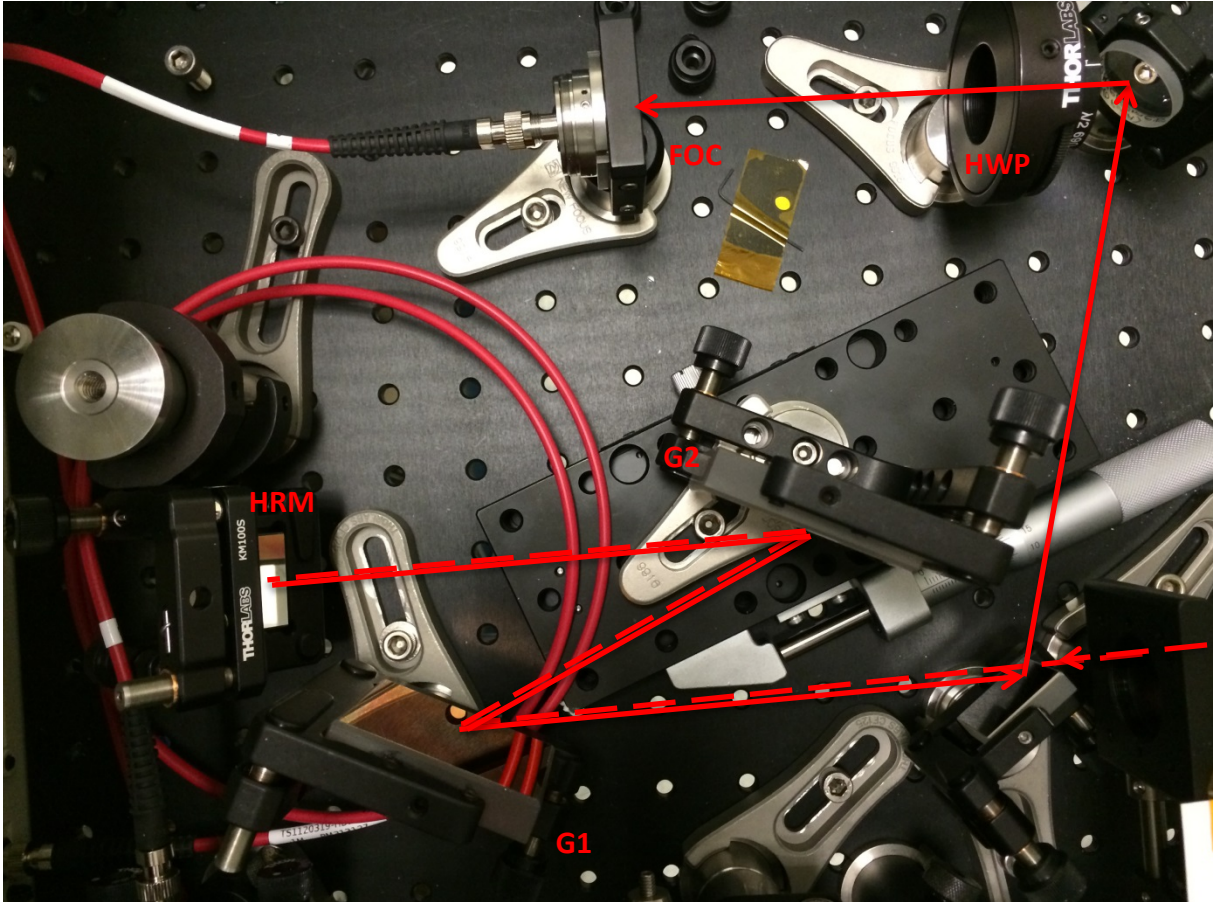


Figure 6. Grating compressor for pre-compensation of dispersion for PM system. G1 and G2 are the gratings, HRM is the hollow roof mirror which shifts the beam vertically down to facilitate beam pickoff, HWP is a half wave plate to set the polarization to match the transmission axis for the subsequent PZ fiber, and FOC is the fiber-optic coupler into the PZ fiber.

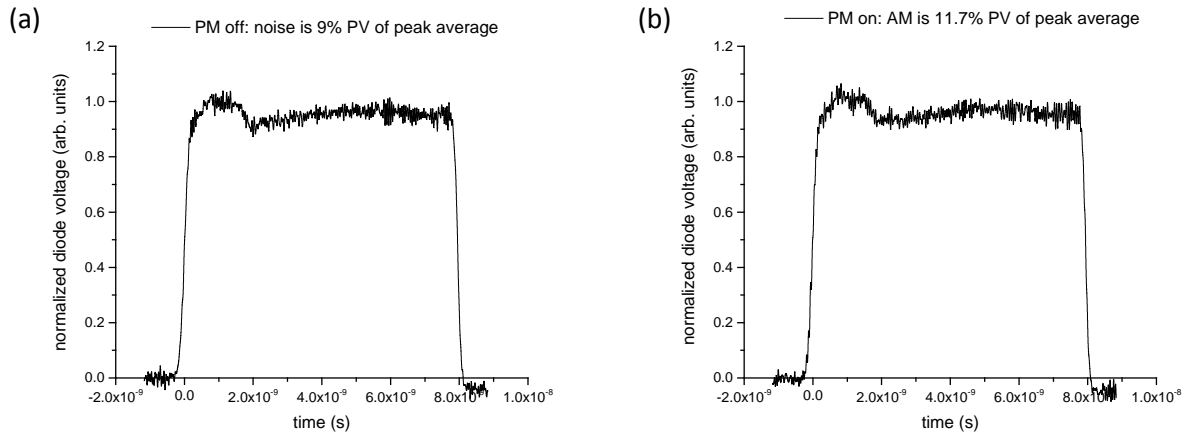


Figure 7. Pre-compensation of dispersion of PZ fiber for PM system. (a) Resulting 30 m PZ fiber output for no PM (and therefore no possible AM) on an 8 ns pulse. (b) Corresponding 30 m PZ fiber output with pre-compensated PM.

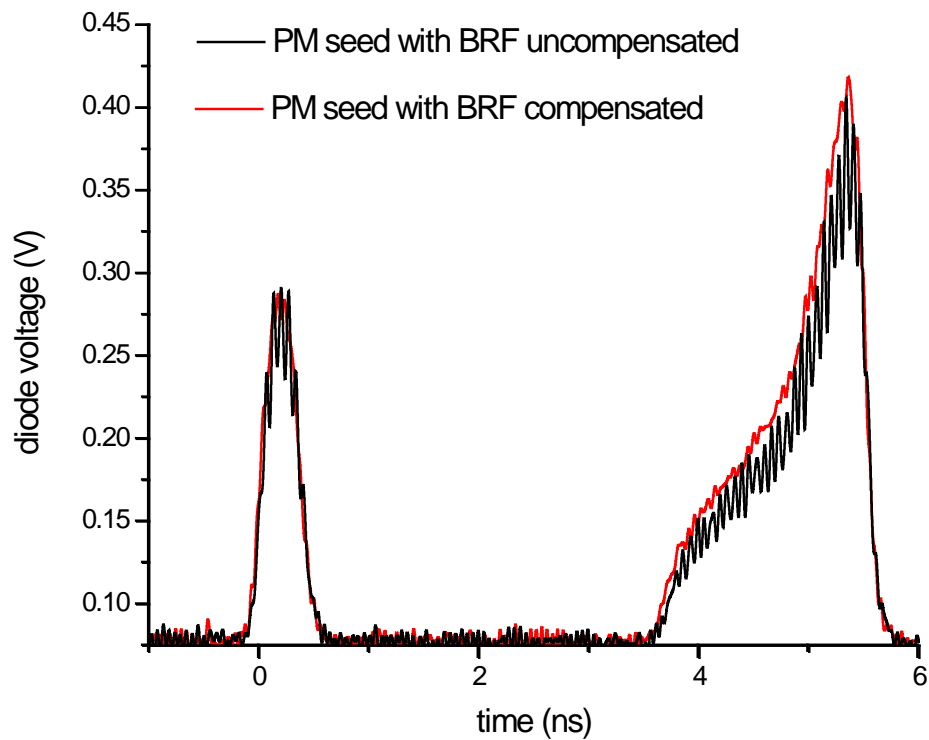


Figure 8. Compensation of spectral amplitude changes in the regenerative amplifier using a BRF.

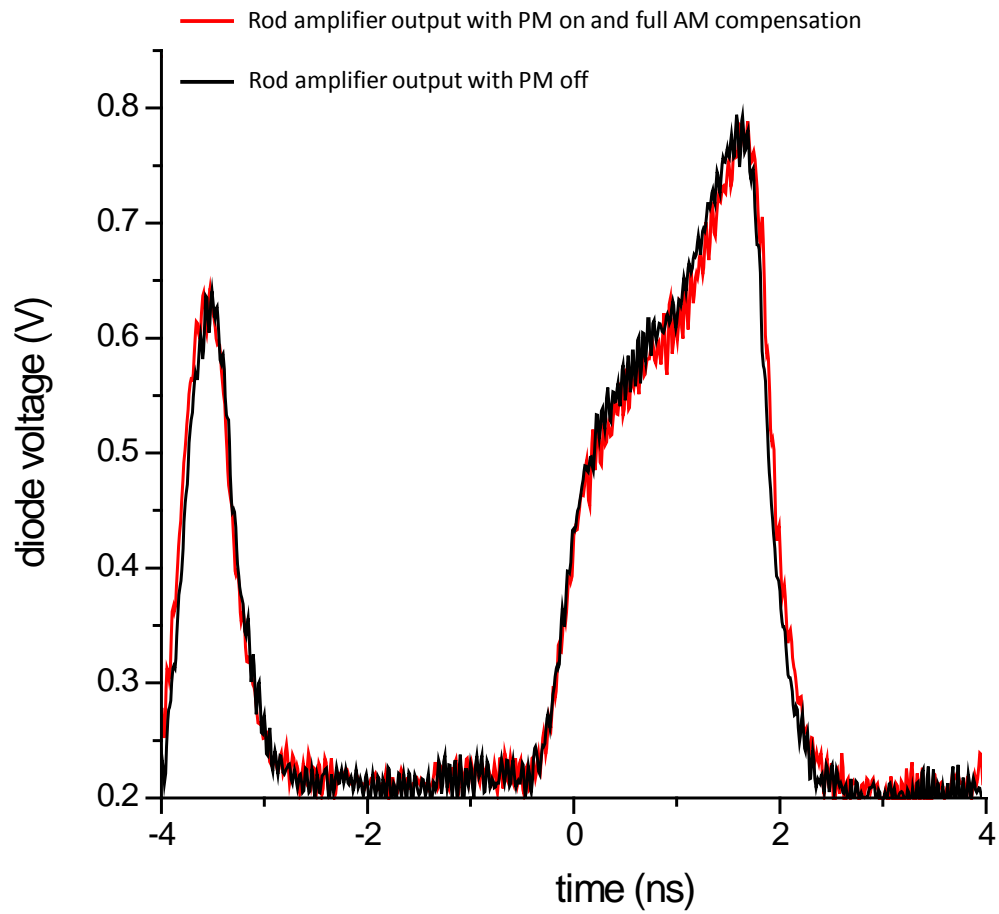


Figure 9. Full compensation of spectral amplitude and phase changes in the 4-pass rod amplifier.

High Energy Data

In running the main 4-pass slab amplifiers for ZBL, there are two key concerns: the creation of transverse SBS and the creation of AM. Both of these can result in damage and/or energy losses if not addressed and monitored. As such, we implemented new diagnostics in two areas: a fast photodiode measurement in the full-aperture 1ω and 2ω diagnostics after the main amplifiers to look for AM (using the same approach as before) and an optical side scatter measurement at the L3 lens (which can pick up the presence of transverse SBS, as seen in [6]).

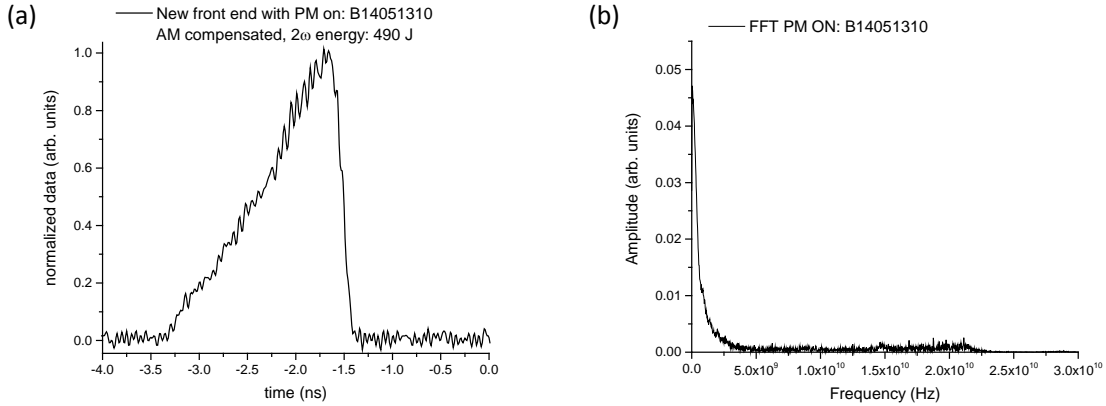


Figure 10. Fast photodiode output at 2ω for a low energy full system shot (below SBS threshold). The left trace (a) is the normalized fast photodiode data while the right traces (b) is the corresponding Fourier transform.

First, we address the AM detection system. Due to the small amount of additional dispersive material and the moderate gain levels (which reduces gain narrowing effects), the main amplifiers themselves are expected to contribute little to AM (as with the 4-pass rod amplifier). However, to verify that the system was being brought up safely, the energy was ramped as we looked at the AM on the fast photodiode data, initially staying below 3 kJ in under 3 ns at 1ω in order to stay below the transverse SBS threshold while looking for any AM caused by PM seed pulses. Figure 10 shows such a low energy shot using the PM seed. Further testing with pulses under 3 ns duration showed minimal levels of AM. This motivated increasing the pulse duration and ramping the energy while continuing to look for any AM. Figure 11 shows the 1ω photodiode data for three successive shots. Note that AM levels on the first and last shots are barely observable but the shot in between had clear low level AM. This was the case throughout the commissioning phase: Generally, there was no observable AM but occasionally there would be a modest observable AM signal (in the 5 to 15% peak-to-valley with respect to peak average). We believe that this periodically observed AM has to do with operational aspects of the system. To clarify, on a daily basis at the regenerative amplifier, the pulsed PM seed level, the operating voltages of the amplifiers, the cavity alignment, the BRG setting, and the associated injected pulse shapes can all be

adjusted to obtain the desired pulse waveform and energy for injection into the subsequent rod and slab amplifier systems. In some cases, the changes are due to environmental issues. All of these can lead to differences in amplifier saturation and associated gain narrowing, which in turn impacts AM. Figure 11 points to this operational variability as the cause for the AM in the fact that the pulshape was clearly adjusted from shot B14052801 to the next shot B14052803, with an accompanying sudden increase in the AM level. The pulse shape stays the same for the subsequent shot B14060301 but the shot occurs the day after the previous two, which likely would have had same subtle differences in settings again.

The second diagnostic was L3 scatter measurement. The spatial filter lenses within ZBL are set up with fiber bundles coupled to the edge of the lens. These are normally connected to a bright light source for illumination required during optic inspection. These fiber bundles are transmissive at 1054nm and can be used to collect side scattered 1ω light onto a diode (100 ps risetime) coupled to a 2.5GHz, 40GS/s oscilloscope. Long wavelength pass color filters (Schott RG850) are used to eliminate observed flashlamp scatter all the way down at L3. L1 data would be more ideal at the moment (as it sees the highest fluence) but flashlamp discrimination and electromagnetic interference there might be very challenging due to the amplifier proximity to the photodiode. As a result, measurements are made at L3. Procedurally, the L3 data are fitted with a 2nd order polynomial along the baseline which is then subtracted. The photodiode trace without baseline is then integrated and normalized to the 1ω laser energy. Changes in this L3 pulshape and its normalized integrated value would be indicative of a nonlinear process like transverse SBS at work. As one can see from Fig. 12, this normalized integrated photodiode value is fairly consistent from shot to shot, indicating that no SBS is present. Unfortunately, since transverse SBS has a threshold condition and is highly nonlinear, the diode will most likely indicate normal behavior or catastrophic failure (unless the energy happens to be in the range right around threshold).

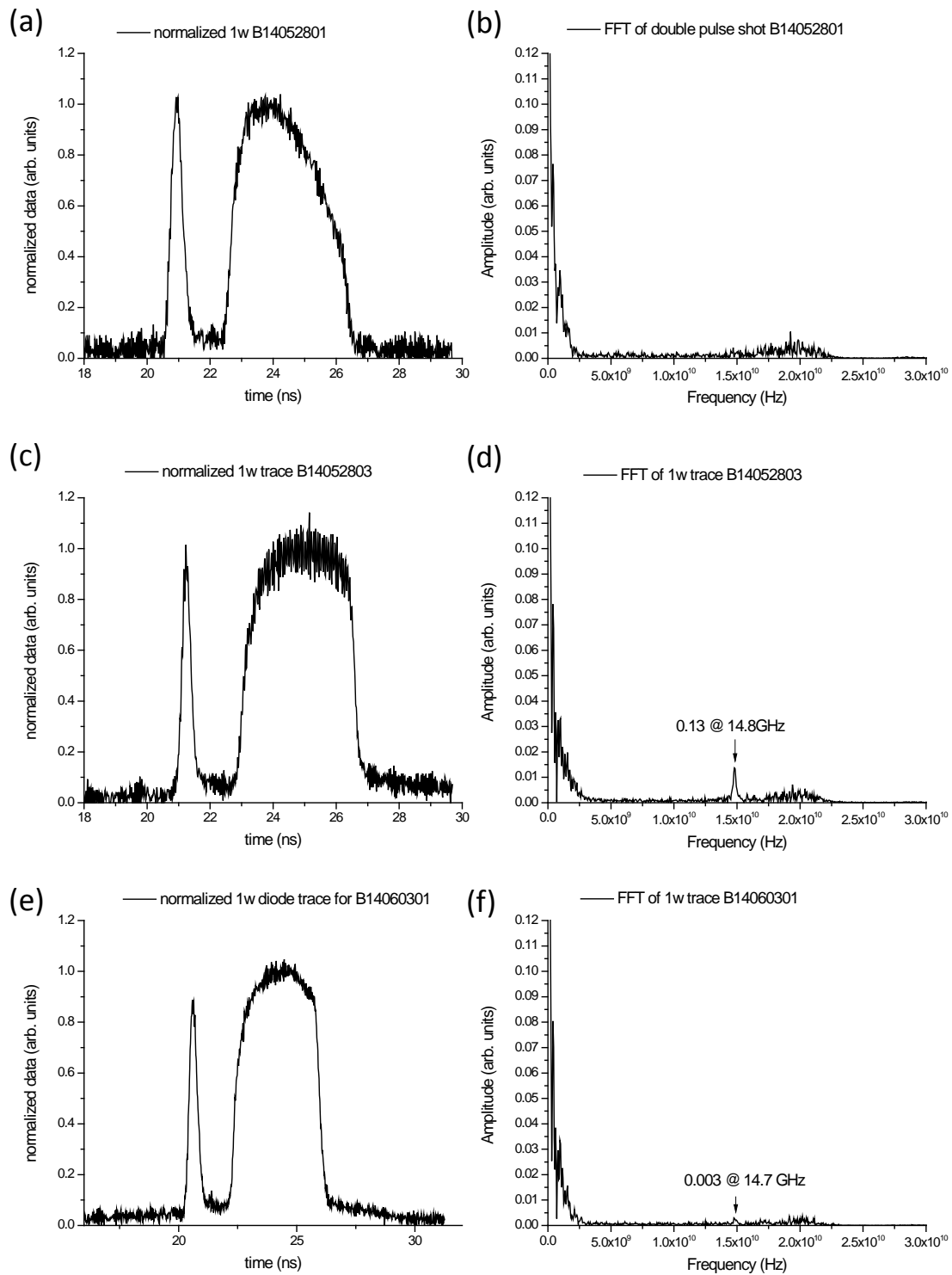


Figure 11. Fast photodiode output at 1ω for three sequential ZBL shots. The left traces (a,c,e) are the normalized fast photodiode data while the right traces (b,d,f) are the corresponding Fourier transforms. The 1ω energies were: 5923 J for B14052801, 5784 J for B14052803, and 5891 J for B14060301.

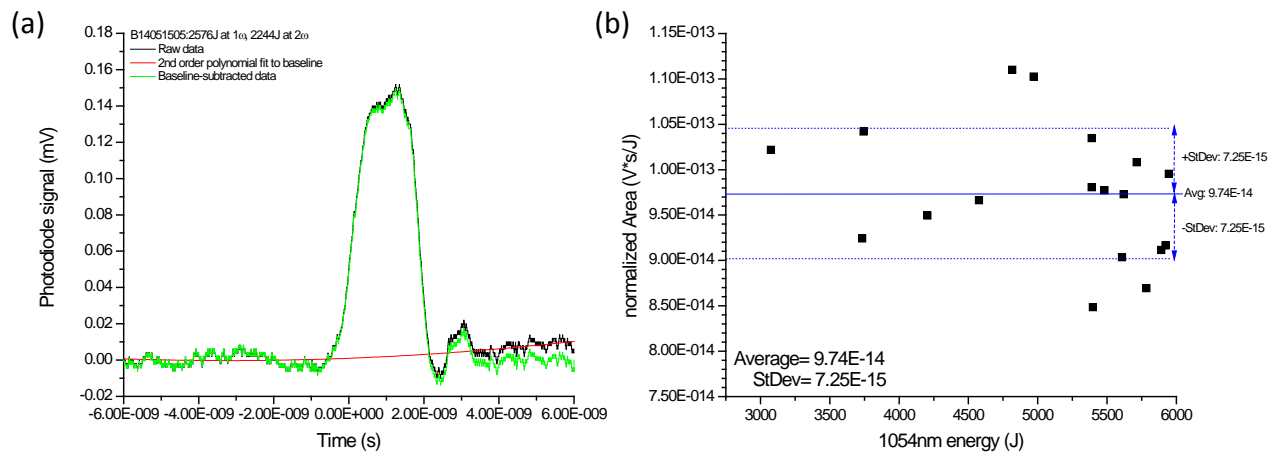


Figure 12. L3 scatter photodiode measurement at 1ω . (a) Representative photodiode trace. (b) Plot of normalized photodiode integral versus energy.

Conclusions

The implementation of a PM seed source and failsafe, along with AM compensation methods, has allowed ZBL to successfully ramp up its energy output. Energies at 1ω prior to the upgrade were typically around 3.5 kJ in a pulsewidth of around 2.5 ns; After the upgrade, 1ω energies can reach greater than 5.5 kJ in 4 ns. More than 20 full system shots have been used successfully with the PM SBSS system. The implementation of the PM system and failsafe is the first element which had to be addressed to increase the available ZBL energy. Upgrades to the shot pinholes and the addition of booster amplifiers would be next on the critical path for further increased laser energy.

References

- [1] P.K. Rambo, I.C. Smith, J.L. Porter, M.J. Hurst, C.S. Speas, R.G. Adams, A.J. Garcia, E. Dawson, B.D. Thurston, C. Wakefield, J.W. Kellogg, M.J. Slattery, H.C. Ives, R.S. Broyles, J.A. Caird, A.C. Erlandson, J.E. Murray, W.C. Behrendt, N.D. Neilsen, and J.M. Narduzzi. Z-beamlet: A multikilojoule, terawatt-class laser system. *Applied Optics*, 44(12):2421–2430, 2005.
- [2] S. A. Slutz, M. C. Herrmann, R. A. Vesey, A. B. Sefkow, D. B. Sinars, D. C. Rovang, K. J. Peterson, and M. E. Cuneo. Pulsed-power-driven cylindrical liner implosions of laser preheated fuel magnetized with an axial field. *Physics of Plasmas*, 17(5):056303–1 to 056303–15, 2010.
- [3] Peter M. Celliers, Kent G. Estabrook, Russell J. Wallace, James E. Murray, Luiz B. Da Silva, Brian J. MacGowan, Bruno M. Van Wonterghem, and Kenneth R. Manes. Spatial filter pinhole for high energy pulsed lasers. *Applied Optics*, 37(12):2371–2378, 1998.
- [4] James E. Murray, David Milam, Charles D. Boley, Kent G. Estabrook, and John A. Caird. Spatial filter pinhole development for the National Ignition Facility. *Applied Optics*, 39(9):1405–1420, 2000.
- [5] J. R. Smith, J. R. Murray, D. T. Kyrazis, R. B. Wilcox, T. L. Weiland, R. B. Ehrlich, C. E. Thompson, R. B. Engle, and A. E. Brown. Acoustic damage to large aperture optics. *Proc.SPIE*, 1047:219–225, 1989.
- [6] J. R. Murray, J. Ray Smith, R. B. Ehrlich, D. T. Kyrazis, C. E. Thompson, T. L. Weiland, and R. B. Wilcox. Experimental observation and suppression of transverse stimulated brillouin scattering in large optical components. *Journal of the Optical Society of America B*, 6(12):2402–2411, 1989.
- [7] B.C. Stuart, M.D. Feit, S. Herman, A.M. Rubenchik, B.W. Shore, and M.D. Perry. Optical ablation by high-power short-pulse lasers. *Journal of the Optical Society of America B (Optical Physics)*, 13(2):459–68, 1996.
- [8] Lawrence Livermore National Laboratories. Advanced conceptual design report for the z-beamlet laser backlighter system. Technical report, Lawrence Livermore National Laboratories, Livermore, CA, 1999.
- [9] R. Wilcox and F. Penko. Optical bandwidth failsafe. *Beamlet Laser Technical Notes*, LST-BLT97-083, 1997.
- [10] Peter J. Wisoff, Mark W. Bowers, Gaylen V. Erbert, Donald F. Browning, and Donald R. Jedlovec. NIF injection laser system. *Proc. SPIE*, 5341:146–155, 2004.

- [11] Alain Jolly, Jean-Francois Gleyze, Denis Penninckx, Nicolas Beck, Laurent Videau, and Herv Coc. Fiber lasers integration for LMJ. *Comptes Rendus Physique*, 7(2):198–212, 2006.
- [12] Mark Bowers, Scott Burkhart, Simon Cohen, Gaylen Erbert, John Heebner, Mark Hermann, and Don Jedlovec. The injection laser system on the National Ignition Facility. *Proc.SPIE*, 6451:64511M–64511M–20, 2007.
- [13] Shuheng Shi, Jifeng Zu, Yong Wang, and Jianqiang Zhu. Research of spacing stability of tunable Fabry-Perot filter in inertial confinement fusion facility. *Chinese Optics Letters*, 5(S1):S56–S59, 2007.
- [14] Steve Hocquet, Denis Penninckx, Edouard Bordenave, Claude Goudard, and Yves Jaoun. FM-to-AM conversion in high-power lasers. *Applied Optics*, 47(18):3338–3349, 2008.
- [15] Jean-Francois Gleyze, Jonathan Hares, Sebastien Vidal, Nicolas Beck, Jerome Dubertrand, and Arnaud Perrin. Recent advances in the front-end sources of the LMJ fusion laser. *Proc.SPIE*, 7916:79160I–79160I–10, 2011.
- [16] Sbastien Vidal, Jacques Luce, and Denis Penninckx. Experimental demonstration of linear precompensation of a nonlinear transfer function due to second-harmonic generation. *Optics Letters*, 36(1):88–90, 2011.
- [17] Huabao Cao, Xingqiang Lu, Linbo Li, Xianhua Yin, Weixin Ma, Jian Zhu, and Dianyuan Fan. Compensation of FM-to-AM conversion in high-power lasers. *Applied Optics*, 50(20):3609–3614, 2011.
- [18] Dangpeng Xu, Zhihua Huang, Jianjun Wang, Mingzhong Li, Honghuan Lin, Rui Zhang, Na Zhu, Yongliang Zhang, and Xiaocheng Tian. A fiber-based polarization rotation filter utilized to suppress the FM-to-AM effect in a large-scale laser facility. *Jour. of Optics*, 15:085702:1–4, 2013.
- [19] Christophe Dorrer, Richard Roides, Robert Cuffney, Andrey V. Okishev, Wade A. Bittle, Gregory Balonek, Albert Consentino, Elizabeth Hill, and Jonathan D. Zuegel. Fiber front end with multiple phase modulations and high-bandwidth pulse shaping for high-energy laser-beam smoothing. *IEEE Journal of Selected Topics in Quantum Electronics*, 19(6):3500112, 2013.
- [20] B. V. Wonterghem. Update on spatial filter implosion. *Beamlet Laser Technical Notes*, LST-BLT96-116, 1996.
- [21] Tayyab I. Suratwala, Jack H. Campbell, William A. Steele, and Rusty A. Steele. Fail safe design for square vacuum-barrier windows. *Proc.SPIE*, 3492:740–749, 1999.
- [22] Darrell J. Armstrong. Operators manual and technical reference for the z-beamlet phase modulation failsafe system: Version 1. *SAND Report*, SAND2014-18120:78, 2014.

- [23] C.P.J. Barty, G. Korn, F. Raksi, C. Rose-Petruck, J. Squier, A.C. Tien, K.R. Wilson, V.V. Yalovlev, and K. Yamakawa. Regenerative pulse shaping and amplification of ultrabroadband optical pulses. *Opt. Lett.*, 21(3):219–221, 1996.

DISTRIBUTION:

- 1 MS 1197 Darrell J. Armstrong, 1682 (electronic copy)
- 1 MS 1197 Ian C. Smith, 1682 (electronic copy)
- 1 MS 1197 Jens Schwarz, 1682 (electronic copy)
- 1 MS 1197 Jonathan Shores, 1682 (electronic copy)
- 1 MS 1197 C. Shane Speas, 1682 (electronic copy)
- 1 MS 1197 John L. Porter, 1682 (electronic copy)
- 1 MS 0899 Technical Library, 9536 (electronic copy)

